ChemComm

Accepted Manuscript

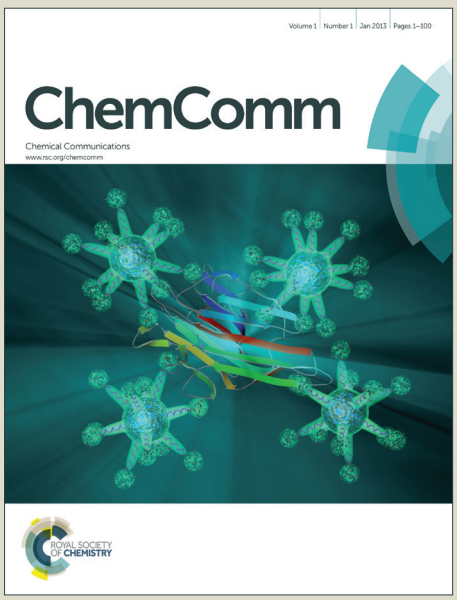

ROYAL SOCIETY OF CHEMISTRY

www.rsc.org/chemcomm

Cite this: DOI: 10.1039/c0xx00000x

www.rsc.org/xxxxxx

ARTICLE TYPE

Enhancing catalytic activity and stability for CO_2 methanation on Ni@MOF-5 *via* controlling active species dispersion

Wenlong Zhen [a,b], Bo Li [a,b], Gongxuan Lu [b,*], Jiantai Ma [a]

Received (in XXX, XXX) Xth XXXXXXXXX 20XX, Accepted Xth XXXXXXXXX 20XX

DOI: 10.1039/b000000x

A novel high active catalyst Ni@MOF-5 showed unexpected higher activity under the low temperature for CO_2 methanation. The characterization results indicated that Ni was in highly dispersed uniform state over MOF-5. This catalyst performed high stability and showed almost no deactivation in long term stability tests up to 100 h.

CO_2 is an inert non-polar compound and the increase of its concentration in the atmosphere has resulted in a profound global climate change [1]. Therefore, CO_2 fixation and conversion have attracted a lot of interests in recent years. CO_2 can be converted into many chemicals, such as CH_3OH [2], DME [3] and CH_4 [4], in which methane maybe the largest amount of hydrogenation product. Methanation of carbon dioxide is a strong exothermal reaction, and can be operated under normal pressure [5]. If the hydrogen needed in this reaction can be obtained *via* an efficient way driven by renewable energy, methanation will be a competitive method to produce methane from CO_2.

Many oxides (SiO_2 and Al_2O_3) supported Ru, Rh and Ni catalysts were reported active for CO_2 methanation[4, 6]. From the point of thermodynamic equilibrium, the low reaction temperature is necessary. In addition, the sintering of active species during reaction can be avoided under low temperature. Furthermore, if the operation temperature is higher than 320°C, the reverse water gas shift (RWGS) reaction undergoes during the reaction, which will leads formation of by-products, such as CO [7].

In order to prepare a high active catalyst for CO_2 methanation, highly uniform dispersed active species over support is required. Usually, it is quite difficult to load enough active species over low specific area supports, although several techniques were explored, such as multi-impregnation with low concentration of salt [4], different precursor, different pH [8] and addition of alkaline elements as anchor connecting components [9]. For example, van Veen et al prepared Ni/Al_2O_3 catalysts with different pH conditions and using different metal salt and alkaline solutions [10]. We also previously reported an active Ni-Ru/γ-Al_2O_3 catalyst (S_{BET}=149.5m^2/g) by different sequential impregnation using low concentration precursors [4]. However, those catalysts cannot prevent the sintering of active species under higher temperature. Therefore, low temperature catalyst is urgently required for CO_2 methanation.

One strategy to prepare low temperature catalyst is usage of high specific surface area support. But the surface areas of normal supports are around 100-200 m^2/g [5]. If the higher surface area support is used, it is possible to prepare high active low-temperature catalyst for CO_2 methanation. Recently, metal-organic frameworks (MOFs) materials emerged as catalyst support because they have very high surface areas, up to more than 1000m^2/g, for example, for hydrogenation of crotonaldehyde [11]. However, MOF-5 supported catalyst has not been explored for heterogeneous CO_2 methanation.

In this work, Ni@MOF-5 was explored as a support for catalyst of CO_2 methanation. Very high dispersion of Ni(41.8%) over MOF-5 (2961 m^2/g) has been achieved in this catalyst. These highly uniform dispersed Ni in the framework in MOF-5 resulted in significant activity enhancement at low temperature. This Ni@MOF-5 catalyst showed almost no deactivation in long term stability tests up to 100 h. Those results imply that MOF-5 is a promising and a novel candidate of support for low temperature catalyst potentially used in CO_2 methanantion.

Catalyst preparation details are described in the ESI.† In order to investigate the influence of reaction temperature and Ni loading on catalytic performance, the xNi@MOF-5 catalysts with different Ni loading (x = 5, 7.5, 10, 12.5) were selected as the representative samples and results were present in Fig. 1A-B. Fig. 1A showed that the CO_2 conversion increased with the reaction temperature increase (from 180 to 320°C) over 10Ni@MOF-5. No CO_2 conversion was found when reaction temperature was below 180°C. However, 10Ni@MOF-5 catalyst showed gradually increase activity when temperature was above 200°C. At the 280°C, the CO_2 conversion reached 47.2%. The selectivity of CH_4 was 100% over the 10Ni@MOF-5 (from 200 to 320°C). CO_2 conversion showed an upward trend when the temperature varied from 200 to 300°C. At the 300°C, the corresponding CO_2 conversion reached 75.1%. This unexpected result indicated that MOF-5 loaded Ni catalyst could catalyse CO_2 methanation under much lower temperature. As a reference, the conversion of CO_2 over 10Ni@SiO_2 sample was about 34% at 280°C under same reaction conditions. In order to study the activity dependence on Ni loading, the comparison tests of all the Ni@MOF-5 catalysts were operated at 280°C.

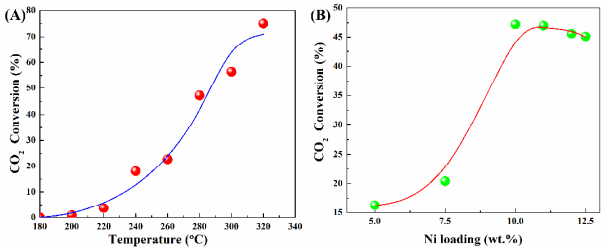

Fig. 1 (A) Effect of temperature on the CO_2 conversion for CO_2 methanation over the 10Ni@MOF-5 catalysts; (B) Effects of Ni loading on CO_2 conversion for CO_2 methanation over xNi@MOF-5 catalyst at 280°C. Reaction conditions: 200 mg catalysts, H_2:CO_2=4:1, GHSV=2000h^{-1}, 1atm.

The effects of Ni loading on CO_2 methanation reactions were present in Fig. 1B. It was clearly shown that increase of Ni loading over MOF-5 led the increase of CO_2 conversion; the maximum reached 47.2% when 10% Ni was deposited over MOF-5 at 280°C. Higher Ni loading might provide more active sites, however, over loading resulted in the segregation of surface Ni particles, which would finally make the activity decrease.

For further understanding the structure and surface state of Ni over MOF-5, the detailed characterizations of XRD, BET, TEM, TPR, XPS, FT-IR and TGA were carried out.

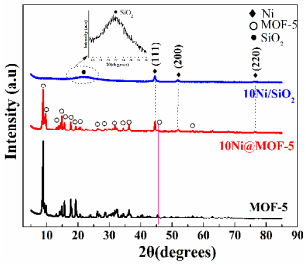

Fig. 2 XRD patterns of the MOF-5, 10Ni@MOF-5 and 10Ni/SiO_2

The typical XRD patterns of the MOF-5, 10Ni@MOF-5 and 10Ni/SiO_2 catalysts were given in Fig. 2. For 10Ni@MOF-5 and 10Ni/SiO_2, the peaks at 44.5, 51.7, and 76.3° were the characteristic peaks of metallic Ni with a face-centered cubic structure (JCPDS# 87-0712). The peaks at 8.9, 9.6, 14.4, 15.7, 17.8, 19.3, 28.7, 31.8, 34.4, 36.3, and 45.5° could be assigned to the diffraction peaks of MOF-5[12], which indicated that our MOF-5 support was well crystalized. The similar intensities of peaks at 51.7 and 76.3° assigned to (200) and (220) facets of Ni. Compared with MOF-5, the Ni signals of 10Ni@MOF-5 (especially at 44.5 and 51.7°) implied the distribution or crystallite size of Ni was similar over MOF-5. From the TEM results(discussed below), the main crystallite size of Ni over 10Ni@MOF-5 was 9.0 nm, while the main Ni particles over 10Ni/SiO_2 were about 42nm as shown in Fig. 3h-i. Almost no particle with diameter larger than 15nm was found over 10Ni@MOF-5 catalyst, however, the ratio of particle with diameter larger than 50nm were over 40% in the 10Ni@SiO_2 catalyst. Besides, according to the Ni content measured by XPS, Ni surface concentration over 10Ni@MOF-5 was 9.73 %, while the datum over 10Ni@SiO_2 was 9.69%, which implied that the difference of Ni dispersion did not resulted from the variation of surface Ni concentration over different supports. In order to further confirm high dispersion of Ni over MOF-5 support, the Ni dispersions over these two samples were measured by H_2 chemisorption. The dispersion of Ni over 10Ni@MOF-5 catalyst was 41.8, while that of Ni dispersion over 10Ni@SiO_2 was 33.7 (See Table S1, ESI†). It indicated that Ni existed in higher dispersion over MOF-5, and this would be identified further by the results of catalytic activity.

The Brunauer-Emmett-Teller specific surface areas (S_{BET}) were determined by N_2 isotherms at 77K (as shown in Table S1, ESI†). The S_{BET} of 10Ni@MOF-5 and MOF-5 were 2961 and 2973 respectively, while that datum of 10Ni@SiO_2 was only 155.6m^2/g. Meanwhile, 10Ni@MOF-5 had larger pore volume which would benefit gas molecule diffusion into the pores.

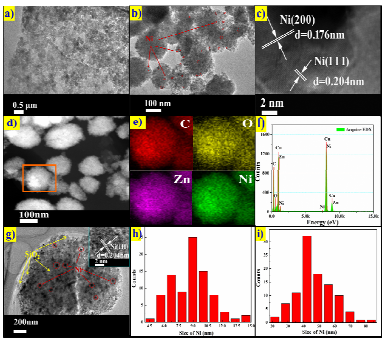

Fig. 3 TEM (a-b), HRTEM (c), HAADF-STEM (d), EDX elemental mapping (e), EDX spectrum (f) and particle size distribution of Ni (h) images of 10Ni@MOF-5; TEM and HRTEM (g) and particle size distribution of Ni (i) images of 10Ni/SiO_2.

In order to better understand the role of Ni in the catalyst, the TEM and HRTEM images of Ni impregnated MOF-5 and SiO_2 were taken (Fig. 3a-i). The morphology and sizes of Ni over MOF-5 was showed in the Fig. 3a-b. Analysis of the Ni nanoparticles (NPs) by high-resolution transmission electron microscopy (HRTEM) images indicated that the d-spacing between two adjacent lattice planes was about 0.204 and 0.176 nm (Fig. 3c). This value was in agreement with the spacing of Ni (111) and (200) planes of face-centered cubic structure. In Fig. 3d-e, the high-angle annular dark field scanning transmission electron microscopy (HAADF-STEM) imaging and energy-dispersive X-ray (EDX) elemental mapping of 10Ni@MOF-5 clearly indicated that the distribution of Ni, Zn, C and O elements were relatively homogeneous in 10Ni@MOF-5. The energy dispersive X-ray (EDX) measurement confirmed the co-existence of Ni, Zn, C and O elements in 10Ni@MOF-5 (Fig. 3f). HRTEM of 10Ni/SiO_2 analysis (see inset in Fig. 3g) revealed the large crystalline features of Ni nanocrystals. From Ni particle size distributions derived from TEM for 10Ni@MOF-5 (Fig. 3h) and 10Ni/SiO_2 (Fig. 3i) catalysts, it was identified that the average crystallite size of Ni over 10Ni@MOF-5 catalyst was smaller than that over 10Ni/SiO_2 catalyst. The lattice spacing of 0.204 nm over SiO_2 support could be indexed to as the (111) plane of face-centered cubic (fcc) Ni lattice, which indicated that the facet over MOF-5 and SiO_2 was almost same.

In order to know the difference of chemical state and reducibility of Ni over different supports [13], H_2-TPR measurements of MOF-5, 10Ni@MOF-5 and 10Ni/SiO_2 catalysts were carried out. The results were given in Fig. 4. It was observed that 10Ni/SiO_2 samples had only one single reduction peak (T_{max}). The T_{max} value of the Ni species was

located at about 414 °C. According to the literature [14], the TPR peak (414°C) was the characteristic reduction of Ni species. There were two reduction peaks over 10Ni@MOF-5 sample, one was around 295°C, and another was centered at 437°C, which was little higher than 414°C. It might due to the stronger metal-support interaction between Ni atom and MOF-5, which did not exist in 10Ni/SiO_2 catalyst [15]. The reduction peak of Ni species over MOF-5 at 295°C reflected that some doped Ni was easily reduced, which provided the active sites under low temperature.

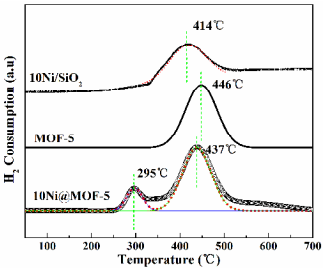

Fig. 4 H_2-TPR profiles of the MOF-5, 10Ni@MOF-5 and 10Ni/SiO_2.

The surface Ni species on 10Ni@MOF-5 and 10Ni/SiO_2 catalysts were examined by XPS measurements, and results were given in Fig. S1a-b (ESI†). The binding energies at 852.6, 870.0, 852.7 and 870.3eV could be assigned to $Ni2p_{3/2}$, $Ni2p_{1/2}$, $Ni2p_{3/2}$ and $Ni2p_{1/2}$, respectively [16]. It indicated that Ni species for 10Ni@MOF-5 and 10Ni/SiO_2 were metallic Ni. Besides, the peak intensity of Ni2p (10Ni/SiO_2) was weak, indicating that the Ni species of 10Ni@MOF-5 was uniformly dispersed in the frameworks. According to the typical XPS survey (wide-scan) spectra of the MOF-5 and 10Ni@MOF-5 in Fig. S1c (ESI†), Ni, Zn, C and O signals confirmed good crystal of used MOF-5.

The typical IR spectra of the MOF and 10Ni@MOF-5 were given in Fig. S2a(ESI†). The MOF and 10Ni@MOF-5 showed the expected strong characteristic adsorptions for the symmetric and asymmetric vibrations of BDC (1580 and 1390 cm^{-1}) and absorption water (3600 cm^{-1}) [17]. 516, 746 and 817cm^{-1} was assigned to absorption peaks of H_2BDC. The Si-O-Si stretching (1125 cm^{-1}) and the Si-O-Si bending (800.3cm^{-1}) frequencies could be recognized [18]. The 3448 and 468.3 cm^{-1} was Si-OH absorption frequencies and Ni-O stretching band, respectively. Those results confirmed the isostructure of the MOF-5 and 10Ni@MOF-5. Thermogravimetric analysis (TGA) curves of MOF-5, 10Ni@MOF-5 and 10Ni/SiO_2 were displayed in Fig. S2b (ESI†). For 10Ni/SiO_2, the weight loss (3.38%) in the temperature ranges from 25 to 110°C due to the loss of water. However, the MOF-5 and 10Ni@MOF-5 had two main steps of weight loss. The first step of weight loss in the temperature range 25-200 °C could be attributed to the loss of water molecules for MOF-5 (17.56%) and 10Ni@MOF-5 (13.25%). The large specific surface area of MOF-5 might result in such amount of water adsorption. The second weight loss began at about 400°C, indicating our MOF-5 was stable below 400°C. When the temperature was higher than 400°C, the decomposition of organic frameworks of MOF-5 underwent [18]. It implied that MOF-5 and 10Ni@MOF-5 had better thermal-stability from 200 to 400°C.

Fig. 5 showed the catalytic activity during 100 h on CO_2 methanation over 10Ni@MOF-5 at 280°C. The stability of a catalyst is closely related to structural destruction, coking and metal sintering during the methanation reaction of carbon dioxides [19-22]. The CO_2 conversion remained above 47.2% and CH_4 selectivity was almost 100% during 80h reaction. Obviously, 10Ni@MOF-5 catalyst was quite stable.

There are different opinions on the nature of the intermediate and the methane formation process. It was previously reported that CO_2 methanation might involve the conversion of CO_2 to CO prior to methanation, and the subsequent reaction followed the mechanism of CO methanation [23]. But other people believed that the methanation might involve the direct hydrogenation of CO_2 to methane without forming CO intermediate [24]. Based on our experiments, the CO generated after 80h test, which suggested that the catalytic mechanism might involve the CO intermediate. Actually, Choe et al. reported that the CO_2 methannation on a Ni(111) surface was initiated by the dissociation of CO_2 into carbon species (CO_{ads}) and oxygen species (O_{ads}) on the Ni surface [25], then CO_{ads} reacted with H to produce CH_4 on Ni(111) [26].

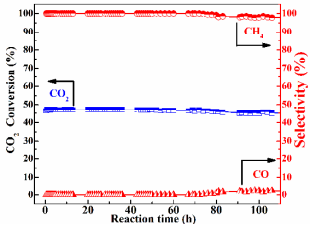

Fig. 5 Long-term (100 h) stability tests over 10Ni@MOF-5 catalyst; reaction conditions: 200 mg catalyst, H_2:CO_2=4:1, GHSV=2000h^{-1}, 1 atm, 280°C.

Above results indicated that the 10Ni@MOF-5 catalyst performed the excellent catalytic activity and stability for CO_2 methantion under the low temperature condition due to the high dispersed Ni active sites over MOF-5. MOF-5 is a promising and a novel candidate of support for low temperature catalyst for CO_2 methanantion.

In summary, a series of high active catalysts Ni@MOF-5 for CO_2 methanation had been prepared by impregnation methods. The 10Ni@MOF-5 showed unexpected higher activity for CO_2 methanation than reference catalyst Ni/SiO_2 under the low temperature (from 180 to 320°C). Based on activity dependence results and the characterization studies of XRD, H_2-TPR, BET, TEM-EDX, XPS, FT-IR and TGA techniques, highly uniform dispersed Ni in the framework in MOF-5 is the main contributor to such significant activity enhancement. For 10Ni@MOF-5, very high specific surface area (2961 m^2/g) and large pore volume (1.037cm^3/g) lead to high dispersion of Ni (41.8%). At 320°C, CO_2 conversion was 75.09% and CH_4 selectivity was 100% over 10Ni@MOF-5. In addition, this 10Ni@MOF-5 catalyst performed high stability and showed almost no deactivation in long term stability tests up to 100 h. MOF-5 is a promising and novel candidate of support for preparation of CO_2 methanantion catalyst.

This work has been supported by the 973 Program and 863 Program of Department of Sciences and Technology China (Grant Nos. 2013CB632404 and 2012AA051501); by the National Natural Science Foundation of China (Grant Nos. 21373245).

Notes and references

[a] *State Key Laboratory of Applied Organic Chemistry, College of Chemistry and Chemical Engineering, Lanzhou University, Lanzhou, China. E-mail: zhenwenlong123@126.com; Tel: +86 931 4968062*

[b] *State Key Laboratory for Oxo Synthesis and Selective Oxidation, Lanzhou Institute of Chemical Physics, Chinese Academy of Science, Lanzhou 730000, China*

** Corresponding author: E-mail: gxlu@lzb.ac.cn. Tel.: +86-931-4968 178. Fax: +86-931-4968 178.*

1 M. Mikkelsen, M. Jorgensen and F. C. Krebs, *Energy Environ. Sci.*, 2010, **3,** 43-81.

2 B. Liaw and Y. Chen, *Appl. Catal., A*, 2001, **206**, 245–256.

3 A. Aguayo, J. Erena, I. Sierra, M. Olazar and J. Bilbao, *Catal. Today*, 2005, **106**, 265–270

4 W. Zhen, B. Li, G. Lu and J. Ma, *RSC Adv.*, 2014, **4**, 16472–16479

5 T. Inui and T. Takeguchi, *Catal. Today*, 1991, **10**, 95–106.

6 G. Weatherbee and C. Bartholomew, *J. Catal.* 1984, **87**, 352–362.

7 X. Xu and J. Moulijn, *Energy Fuels*, 1996, **10**, 305–325

8 J. Dawody, M. Skoglundh, S. Wall and E. Fridell, *J. Mol. Catal. A: Chem.,* 2005, **225**, 259–269

9 Y. Nagai, T. Hirabayashi, K. Dohmae, N. Takagi, T. Minami, H. Shinjoh and S. Matsumoto, *J. Catal.*, 2006, **242,** 103–109.

10 G. van Veen, E. Kmissink, E. Doesburg, J. Ross and L. van Reijen, *React. Kinet. Catal. Lett.*, 1978, **9**, 143-148.

11 H. Zhao, H. Song and L. Chou, *Inorg. Chem. Commun.* 2012, **15**, 261–265

12 K. Sugikawa, S. Nagata, Y. Furukawa, K. Kokado and K. Sada, *Chem. Mater.*, 2013, **25**, 2565−2570

13 C. Hu, J. Yao, H. Yang, Y. Chen and A. Tian, *J. Catal.*, 1997, **166**, 1-7.

14 K. Hadjiivanov, M. Mihaylov, D. Klissurski, P. Stefanov, N. Abadjieva, E. Vassileva and L. Mintchev, *J. Catal.*, 1999, **185**, 314-323

15 H. S. Roh, W. S. Dong, K. W. Jun, Z. W. Liu, S. E. Park and Y. S. Oh, *Bull. Korean Chem. Soc*., 2002, **23,** 669-673

16 G. Wu, X. Tan, G. Li, and C. Hu, *Chem. Res. Chin. Univ.*, 2013, **29**, 154-158

17 L. Huang, H. Wang, J. Chen, Z. Wang, J. Sun, D. Zhao and Y. Yan, *Microporous Mesoporous Mater.*, 2003, **58**, 105–114

18 R. Hofman, J. G. F. Westheim, J. Pouwel, T. Fransen and P. J. Gellings, *Surf. Interface Anal.,* 1996, **24**, 1-6.

18 H. Li, W. Shi, K. Zhao, H. Li, Y. Bing and P. Cheng, *Inorg. Chem.,* 2012, **51,** 9200−9207

19 R. Razzaq, C. Li, M. Usman, K. Suzuki and S. Zhang, *Chem. Eng. J.*, 2015, **262**, 1090-1098;

20 P. Ussa Aldana, F. Ocampo, K. Kobl, B. Louis, F. Thibault-Starzyk, M. Daturi, P. Bazin, S. Thomas and A. Roger, *Catal. Today,* 2013, **215**, 201-207;

21 J. Li, L. Zhou, P. Li, Q. Zhu, J. Gao, F. Gu and F. Su, *Chem. Eng. J.*, 2013, **219**, 183-189

22 J. Li, L. Zhou, Q. Zhu and H. Li, *Ind. Eng. Chem. Res.*, 2013, **52**, 6647-6654

23 A. Lapidus, N. Gaidai, N. Nekrasov, L. Tishkova, Y. Agafonov and T. Myshenkova, *Pet. Chem*., 2007, **47**, 75–82.

24 S. Fujita, H. Terunuma, H. Kobayashi, N. Takezawa, *React. Kinet. Catal. Lett.*, 1987, **33**, 179–184.

25 M. Jacquemin, A. Beuls and P. Ruiz, *Catal. Today,* 2010, **157,** 462-466

26 C. Swalus, M. Jacquemin, C. Poleunis, P. Bertrand and P. Ruiz, *Appl. Catal., B.*, 2012, **125**, 41-50.